

# Investigation into Ultra-High Molecular Weight Polyethylene/Modified Nano-Zinc Oxide Nanocomposites

Haydar U. Zaman<sup>\*1</sup>, Ruhul A. Khan<sup>2</sup>

<sup>1</sup>National University of Bangladesh and Senior Researcher of Institute of Radiation and Polymer Technology, Bangladesh Atomic Energy Commission, Savar, Dhaka, Bangladesh

<sup>2</sup>Institute of Radiation and Polymer Technology, Bangladesh Atomic Energy Commission, Savar, Dhaka, Bangladesh

**ABSTRACT:** It is easier to exhibit appropriate mechanical and chemical properties when nano-zinc oxides are introduced to polymers as reinforcement, generating a completely flexible designed composite. Polymer mixtures are a vital component in the management of novel materials, which excel above net polymers in terms of characteristics. Polymer blends are able to provide substances with long-lasting beneficial properties, which is different from what can be achieved with a single polymer equivalent. In this study, modified zinc oxide nanoparticles (nZnO) reinforced ultra-high molecular weight polyethylene (UHMWPE) reinforcement was tested to see how varied filler loadings (0.1–0.7 wt %) would affect the mechanical, melt rheological, and antibacterial performances. UHMWPE and 3-aminopropyltriethoxy silane-modified nano-ZnO were combined to create UHMWPE/nZnO nanocomposites utilizing a dry mechanical ball mill and compression molding. The study's conclusions revealed that the UHMWPE nanocomposites' mechanical properties were improved by the addition of modified nano-ZnO. The tensile properties, such as compressive strength, tensile strength, compressive modulus, elongation at break, and Vickers microhardness, were altered by the concentration of modified nano-ZnO. As filler loading was increased, the compressive strength and modulus, tensile modulus, and Vickers micro-hardness of nano-ZnO/UHMWPE composites all improved. When nano-ZnO was added to UHMWPE, the tensile strength and elongation at break were yet reduced. The maximum tensile strength and elongation at break were achieved with modified nano-ZnO at a concentration of 0.5 wt%. The nanocomposites showed promising antibacterial activity when tested against *Escherichia coli* and *Staphylococcus aureus*. The low doped level of modified nano-ZnO in the UHMWPE matrix led to a little increase in the melt viscosity of the composites.

**KEYWORDS:** Nanocomposites, UHMWPE, modified nano-ZnO, antibacteria, mechanical properties, melt viscosity

<https://doi.org/10.29294/IJASE.9.3.2023.2848-2856> ©2023 Mahendrapublications.com, All rights reserved

## INTRODUCTION

Many modern high-tech engineering materials are made of polymers with a range of reinforcements, such as short fibers, minerals, organic compounds, and inorganic elements. These polymer composites have a number of advantages over metals and ceramics, including simplicity of manufacture, light weight, low cost, and comparable mechanical strength. Ultra-high molecular weight polyethylene (UHMWPE), one of the most significant commercialized polymers, has a number of high-performance and unique characteristics, including biocompatibility, chemical inertness, excellent impact strength [1, 2], and the highest abrasion resistance in comparison to other thermoplastics [3]. It began to eclipse traditional

PE in popularity when Sir John Charnley used it as an implant material for human joints for the first time in 1970. UHMWPE components are used as human joint implants to successfully treat a variety of joint diseases, such as rheumatoid arthritis and osteoarthritis. Along with the components of artificial implants, it is extensively used in other industrial applications such as engineering bearing, valve, vehicle parts, etc. Its low surface hardness, insufficient creep resistance, and low elastic modulus continue to be major problems despite their increased attention.

Since they typically exhibit morphological, mechanical, and thermal features, organic-inorganic composites have recently attracted

*\*Corresponding Author: haydarzaman07@gmail.com*

Received: 10.12.2022

Accepted: 28.01.2023

Published on: 04.02.2023

Haydar U Zaman & Ruhul A Khan

the attention of scientists. This interest has been largely focused on nanocomposites. Modifying polymers using inorganic particle fillers might enhance their mechanical and thermal properties while also on occasion bringing down their price. The properties of the composites are significantly influenced by the size, shape, type, surface characteristics, and degree of dispersion of the organic/inorganic fillers [4-7]. A new path has been opened up for the advancement of polymer technology with the addition of inorganic nanoparticles to polymers. Inorganic nanoparticles can significantly alter the mechanical properties of the polymer matrix due to their high surface to volume ratio and other advantageous characteristics like thermal and electrical conductivity. As a result, as compared to traditional polymer additives, it offers more advantages in terms of its physical, mechanical, and other functional properties. Inorganic nanoparticles including  $ZrO_2$ [8],  $SiO_2$ [9],  $CuS$  [10],  $ZnO$  [11],  $CuO$  and  $TiO_2$ [12] have been reported to improve the mechanical and tribological properties of polymer matrix materials. The primary determining factors of the properties of particulate-filled polymer composites are the filler types, filler loading, and interactions between the filler and matrix [13]. One of the multifunctional inorganic nanoparticles, nano-ZnO, has received more attention lately. Because of the substance's many notable physical and chemical characteristics, including its high chemical stability, low dielectric constant, high electromechanical coupling coefficient, high luminous transmittance, high catalytic activity, intense ultraviolet and infrared absorption, etc. Therefore, nano-ZnO can be utilized to create UV-blocking materials, [14], semiconductors [15], varistors [16], gas sensors [17], piezoelectric devices [18], and catalysts [19], among other things. Exceptional strength, toughness, electrical conductivity, optical, and bacterial resistance characteristics are found in ZnO, a recently discovered reinforcing material [20-22]. The incorporation of nano-ZnO into polymers may improve their mechanical and optical properties because of the potent interfacial interaction between the organic polymer and the inorganic nanoparticles, the nanoparticles' enormous specific area and small size, as well as the quantum effect. Because of this, these nanocomposites could be applied to a variety of various things, such as coatings, rubber, plastics, sealants, textiles, and more [23,

24]. Several researchers have conducted a great deal of study on nano-ZnO-reinforced polymer composites. According to studies on micro- and nano-ZnO-filled polypropylene (PP) composite by Subramani et al., [25], ZnO demonstrates exceptional antibacterial action against two different human pathogenic bacteria, the *Staphylococcus aureus* (*S.aureus*) and the *klebsiella pneumonia*. With the addition of a small amount of ZnO nanoparticles, Li et al. [26] observed that linear low-density polyethylene (LLDPE) film's mechanical properties had also enhanced with the addition of a modest amount of ZnO nanoparticles. ZnO nanoparticles are crucial in a variety of polymer matrixes, as other studies have conclusively shown [11, 27, 28]. It's interesting that nothing has been reported regarding how ZnO-nanoparticles alter UHMWPE's properties. In order to increase UHMWPE's suitability for biomedical applications such artificial joint replacements, ZnO-nanoparticles, which are widely known for being biocompatible materials and antibacterial agents, could be added.

UHMWPE enhanced with ZnO nanoparticles was created in this study using a dry mechanical ball mill and compression molding. To improve the compatibility of nano-ZnO and UHMWPE matrix, 3-aminopropyltriethoxysilane was used as a coupling agent. Investigations were made to determine how the changing nano-ZnO concentration influenced the mechanical, melt rheological, and antibacterial performances of the composite films.

## EXPERIMENTAL

### Materials Used

The molecular weight of the UHMWPE grade GUR 4120, which has a density of  $0.93 \text{ g/cm}^3$ , is  $5 \times 10^6 \text{ g/mol}$ , and it was purchased from Tianjin Petroleum & Chemical Corporation in China. Commercially available ZnO nanoparticles from the Nanjing, China-based HT Nano-materials Corporation were used in their precise form, with an average diameter of roughly 50 nm. The Shuguang chemicals firm in Nanjing, China, created 3-aminopropyltriethoxysilane ( $C_9H_{23}NO_3Si$ ), a surface modification. The other reagents, analytical-grade items, were purchased from a chemical supply shop.

## PROCEDURES

### UHMWPE/Nano-ZnO Nanocomposites Fabrication

Figure.1 depicts the surface modification procedure for ZnO nanoparticles. Silane-treated ZnO nanoparticles were produced after being oven at 100°C to dry them out. Using a dry mechanical ball mill, ZnO nanoparticles were combined with UHMWPE at various filler loadings ranging from 0 to 0.7 wt%. The milling procedure took 4 hours to finish, with 2 hours spent in each of the clockwise and

counterclockwise directions. The mixture was then put to a 90 × 90 × 9 mm<sup>3</sup> mold after mixing. The samples underwent a 10-minute preheating period and a 15-minute hot pressing process at 160°C. The nano-ZnO/UHMWPE composite was produced after cooling to ambient temperature. After that, the composites were trimmed and cut into the proper dimensions for testing.

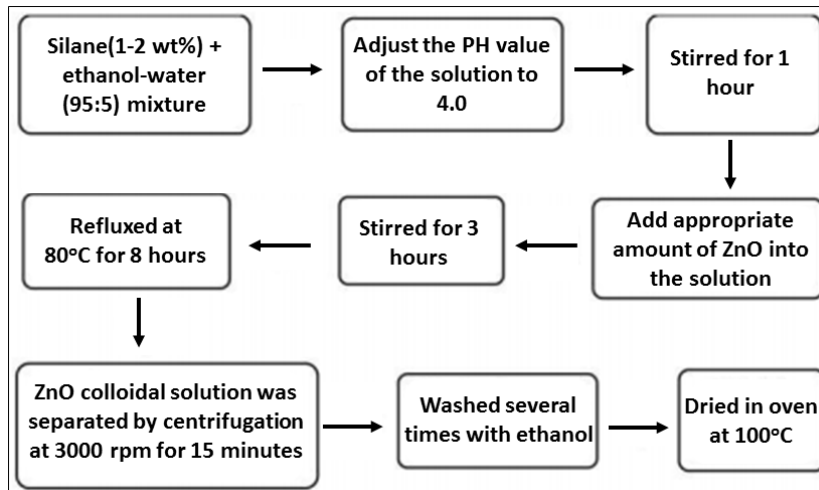


Figure 1: Surface of the nanoparticles has been coated with ZnO

## CHARACTERIZATIONS

### Measurement of Mechanical Features

To assess the mechanical characteristics of the pure UHMWPE and nano-ZnO/UHMWPE composites, compression, tensile, and micro-hardness tests were performed. Using an Instron 3360 universal testing machine, compression and tensile tests were conducted. Compression samples had a 9 mm × 9 mm × 25 mm<sup>3</sup> size with a 25 mm compression length (l). All of the samples had an average l/d ratio of about 2.8, which causes a double-barreling deformation. Unless an early failure occurs, all tests were conducted with a crosshead speed of 5 mm/min up to a compression displacement of 10 mm. The stress-strain curves were used to calculate the mean and standard deviation of compressive strength and modulus for five samples. Tensile test results were calculated using ASTM D638 (Type IV) with a 5 mm/min crosshead speed. The stress-strain graphs were used to calculate the mean and standard deviation of the tensile strength, tensile modulus, and elongation at break for 5 samples. The Shimadzu micro-hardness tester Type-M was used to conduct the micro-hardness test.

From the following equation, the Vickers micro-hardness number ( $H_{mv}$ ) was determined:

$$H_{mv} = 1854.4 \times \frac{P}{d^2} \quad (1)$$

where d is the diagonal length measurement of the pyramidal indentation on the sample surface (μm), and P is the test load on the diamond indenter (g). The test load for the micro-hardness indentation on the sample's surface was 50 g, and the indentation time was 10s. For the purpose of calculating the mean and standard deviation, each sample was subjected to a total of six measurements.

### Morphological Observation

Scanning electron microscopy was used to analyze the nanocomposites' morphology (JSM-6380 SEM, JEOL Ltd., Tokyo, Japan). Before analysis, the samples were sputter-coated with gold after being freeze-fractured in liquid nitrogen.

### Antibacterial Evaluation

The plate-counting approach was used to assess the antibacterial effects on *Escherichia coli* (ATCC10536, *E. coli*) and *Staphylococcus aureus* (ATCC6538, *S. aureus*) [29]. To

completely eliminate any microorganisms on the surface, 70% ethanol was initially used to wash the samples (5 cm × 5 cm). After drying, 0.2 ml of a bacterium solution ( $2.0\text{--}5.0 \times 10^6$  cells per ml) was added to the film surface. A UHMWPE film (4 cm × 4 cm) was then applied to the surface. These carrier films were stored at or below 37°C and at or above 90% relative humidity. After 24 hours, the bacteria were removed using a 0.80% NaCl solution, and 1 ml of this suspension was serially diluted before being plated onto nutritional broth agar (NA). The bacteria's colony forming units (CFU) were counted, and the antibacterial rate (R) was determined using the equation shown below [30]:

$$R(\%) = \frac{B - C}{B} \times 100 \quad (2)$$

where C is the CFU of the antibacterial samples, R is the antibacterial rate, and B is the CFU of the blank sample.

### Measurement of Capillary Rheology

Using a capillary rheometer (RH2000, Rosand Precision, UK) and shear rates ranging from 20 to 3000 s<sup>-1</sup>, capillary rheological properties were examined at five different temperatures (150, 155, 160, 165, and 170°C). The capillary had a diameter of 1 mm and a length to diameter ratio (L/D) of 35 mm. Prior to measurement, the samples were warmed at a test temperature for 5 min. By applying the standard equation to the experimental data, the apparent shear viscosity ( $\eta_a$ ) and apparent shear rate ( $\dot{\gamma}_w$ ) were computed [31]. The Bagley correction is disregarded since the capillary's L/D ratio is 35. For non-Newtonian behavior, the Rabinowitsch adjustment was applied.

## RESULTS AND DISCUSSION

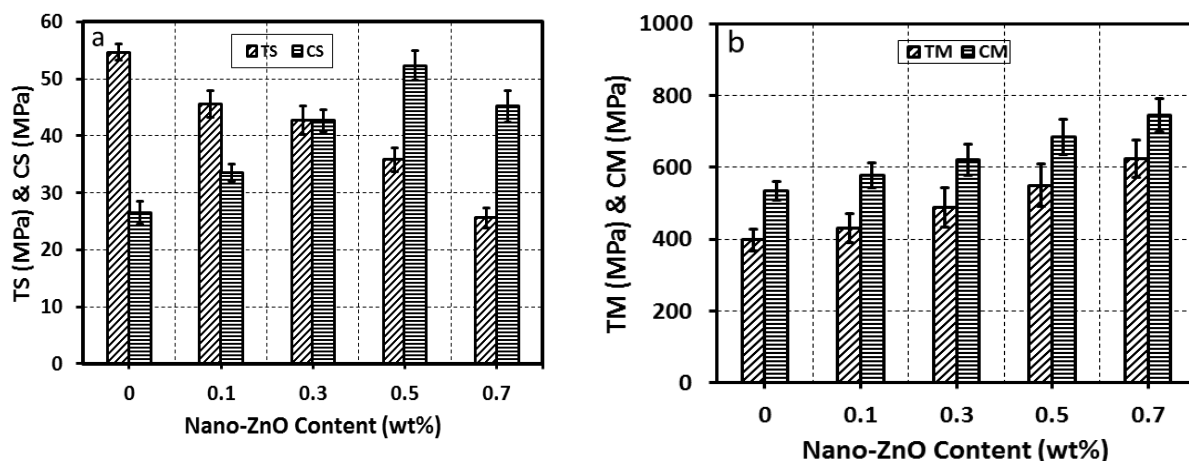
### Mechanical Features

Figure 2 shows the nano-ZnO/UHMWPE composites' compressive strength, tensile strength, compressive modulus, tensile modulus, elongation at break, and microhardness as a function of filler loading. The compressive strength rises for loadings of 0.1, 0.3, 0.5, and 0.7 wt% nano-ZnO filler, as shown in Figure 2(a). The compressive strength reaches its maximum value of 52.3 MPa at a filler loading of 0.5 weight percent nano-ZnO. The increase is nearly 97% more than the

strength of pure UHMWPE (26.5 MPa). When 0.7 weight percent of nano-ZnO is loaded, the compressive strength is significantly reduced. Compression behavior is a critical factor to take into account when deciding which materials to utilize for load-bearing systems that are constantly under pressure. As a result of the samples being squeezed and deformed, submicroscopic cracks will develop in the UHMWPE matrix. The submicroscopic fissures in the UHMWPE matrix may be filled by the nano-ZnO filler under stress. The inclusion of hard fillers will further restrict the chain's mobility and deformation due to the frictional force of the particles. After the nano-ZnO filler is added, the stress capacity of the composites is increased, leading to higher compressive strength. The reduction in compressive strength at 0.7 wt% shows that agglomeration in the composite system is brought on by a decrease in the efficiency of stress transfer between nano-ZnO and UHMWPE as a result of the reduction in filler inter-particle distance at higher filler loading. In contrast, as nano-ZnO content is raised, the tensile strength of nano-ZnO/UHMWPE composites tends to decrease. The influence of nano-ZnO reinforcement in UHMWPE was less significant under tension compared to compression mode. It is well known that the tensile strength of polymer composites is significantly influenced by the adherence of the filler and matrix at their interface. The lower tensile strength found in this study shows that there is inadequate adhesion between the nano-ZnO and the UHMWPE matrix to promote stronger interfacial bonding, which would raise the tensile strength value. The silane concentration utilized, which was 1 wt% but may not be at the ideal level to increase tensile strength, may be partially to blame for this. It is necessary to look into the optimal silane loading in this composite system in more detail.

The tensile and compression moduli of nano-ZnO/UHMWPE composites are shown in Figure 2(b) as functions of filler loading. The tensile and compressive modulus of UHMWPE is typically increased nonlinearly by ZnO nanoparticles. Tensile and compressive modulus was increased by 56% and 40%, respectively, when 0.7 weight percent of ZnO nanoparticles were added to the UHMWPE matrix. This is caused by the proliferation of rigid ZnO nanoparticles in the UHMWPE matrix. The composites' rigidity and stiffness increased as the filler loading was raised as a result.





**Figure 2: Tensile characteristics of nano-ZnO/UHMWPE nanocomposites as a function of filler loading: (a) tensile strength (TS) and compressive strength (CS); (b) tensile modulus (TM) and compressive modulus (CM)**

The decrease in elongation at break of UHMWPE caused by the addition of nano-ZnO is seen in Figure 2(c). This indicates that the ductility and level of plastic deformation reduced as the nano-ZnO loadings increased. The variations in surface hardness and tensile modulus were determined according to the internal structure of the bulk and unique surface properties respectively. Figure 2(d) illustrates the Vickers micro-hardness of composites made of nano-ZnO and UHMWPE. The Vickers micro-hardness number slowly increased after nano-ZnO was added to the UHMWPE matrix, as is evident. Vickers micro-hardness increases by 47% as compared to pure UHMWPE, reaching its peak value at 0.7 weight percent filler loading. The increase in micro-hardness may be brought on by the rigid nano-ZnO fillers in the polymer. Any plastic distortion during the indentation was avoided due to the addition of nano-ZnO fillers. As more nano-ZnO fillers were loaded, the gap between the fillers would get smaller. As a result, it was observed that the Vickers micro-hardness number increased with increasing nano-ZnO filler loadings.

During the modification process, the silane coupling agents and the surface of the nanoparticles are stated to go through a hydrolysis and condensation reaction in a polar solution [32]. The hydrophilic surface of the nanoparticles is partially changed to a hydrophobic one by the silane bonding, which removes the hydroxyl groups from the nanoparticles' surface. Decreased nanoparticle-nanoparticle interaction and improved nanoparticle dispersibility in the polymer

matrix are the end consequences of the surface treatment.

Therefore, the reduction of nanoparticle-nanoparticle contact and improvement of the dispersibility of the nanoparticles in the polymer matrix are the results of the surface treatment. Thus, as shown in Figure 3b, the nanoparticles exhibit good dispersibility in the composite films at a relatively low modified nano-ZnO content, which led to an improvement in the composite films' elongation at break and tensile strength. The aggregation of the nanoparticles may be the cause of the ZnO particles in the UHMWPE matrix enlarging in size when the content of modified nano-ZnO increases further, as seen in Figure 3(c, d). Nano-ZnO particle aggregation can result in a reduction in the contact area between the nanoparticles and the matrix and flaws in the composite films. As a result, the mechanical characteristics of the composite films were reduced due to the relatively high proportion of nano-ZnO.

### Antibacterial Features

The outcomes of antibacterial tests on UHMWPE/modified nano-ZnO nanocomposites are shown in Figure 4. With an antibacterial rate of less than 7% against *Escherichia coli* and *Staphylococcus aureus*, respectively, pure UHMWPE film is clearly virtually completely devoid of antibacterial action. However, as the amount of nano-ZnO in the composite films grew, the antibacterial rate also did so. The antibacterial rate against *Escherichia coli* is 85.6%, and against *staphylococcus aureus*, it is 88.9% when the nano-ZnO content is 0.7 wt%.

The antibacterial activity of nano-ZnO particles is responsible for the composite films' good antibacterial characteristics. The antibacterial activity of ZnO was thought to be caused by the following potential causes: the first is that when  $\text{Zn}^{+2}$  released by ZnO contacts with the cell membranes of microbes, the cell membranes' negative electricity and  $\text{Zn}^{+2}$ 's positive electricity attract one another. The  $\text{Zn}^{+2}$  would

then penetrate the cell membranes and react with sulfhydryl inside the cell membranes. As a result, the microbe's ability to produce synthetase is severely compromised, which causes the cells to lose their capacity for cell division and development and ultimately cause the microbe to death. The production of hydrogen peroxide ( $\text{H}_2\text{O}_2$ ) from ZnO surfaces may also play a role [33].

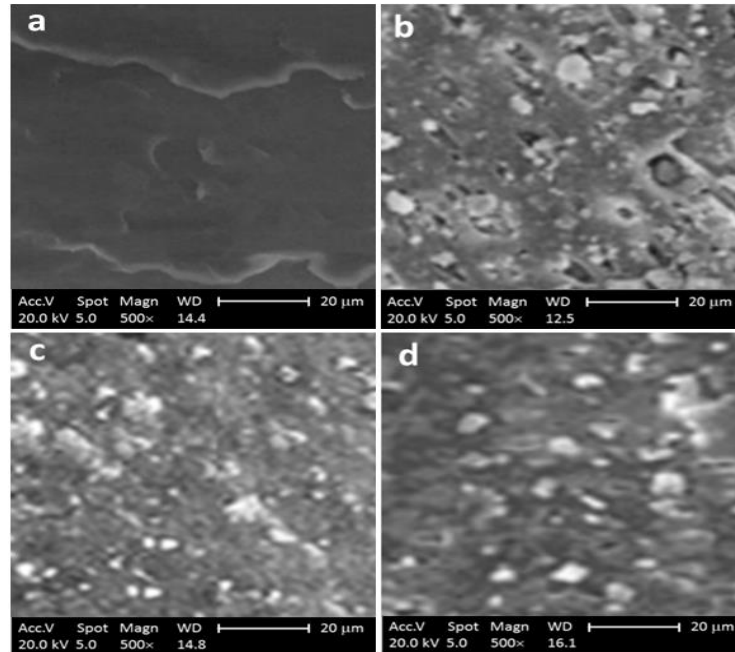


Figure 3: SEM images of UHMWPE/modified nano-ZnO nanocomposites with the following nano-ZnO content (wt%) values: (a) 0, (b) 0.3, (c) 0.5, and (d) 0.7

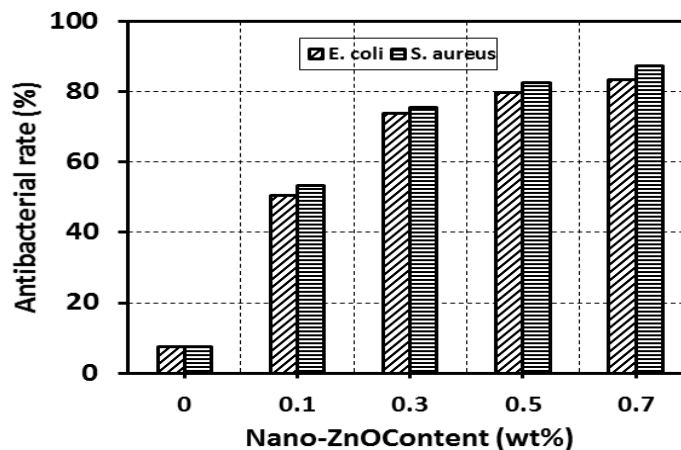


Figure 4: Films made of UHMWPE and modified nano-ZnO has a high antibacterial rate against *S. aureus* and *E. coli*

#### Features of Capillary Rheology

Figure 5 depicts logarithmic graphs of the melt viscosity of the UHMWPE/modified nano-ZnO composite versus the shear rate at 170°C. The melt viscosity clearly decreases with an increase in shear rate when the nano-ZnO concentration is constant, demonstrating that the melts of all these samples are pseudoplastic

fluids with shear-thinning flow behavior and follow the equation of a fluid with a power-law relationship. It has to do with a change in molecular state brought on by shear, which is typically explained in terms of molecular chain entanglement [34]. Due to the entanglement density falling as the shear rate increases, the melt is shear thinned. The melt viscosity of

UHMWPE/modified nano-ZnO nanocomposites, on the other hand, is slightly higher at a constant shear rate than that of pure UHMWPE, and it also slightly rises with an increase in the nano-ZnO concentration. The interfacial interaction between resin and nanoparticles at a rather low modified nano-ZnO level is mostly

to blame for this. A further rise in the quantity of modified nano-ZnO causes an increase in the interfacial contact as well as the melt viscosity, which is attributable to the ZnO particles rubbing up against one another as a result of the aggregation of nano-ZnO particles [35].

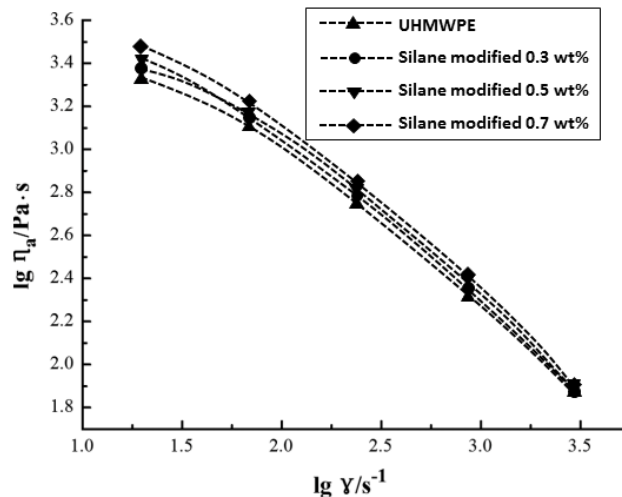


Figure 5: Melt flow curves of composites made of UHMWPE and modified Nano-ZnO at 170°C

Figure 6 depicts the relationship between the temperature and the melt viscosity of the composites at a 242 s<sup>-1</sup> shear rate. The figure shows that as temperature rises, melt viscosity

falls. Because the contact between the chains shrinks and the free volume of the melt expands as the temperature raises, the chain segment's ability to move is enhanced.

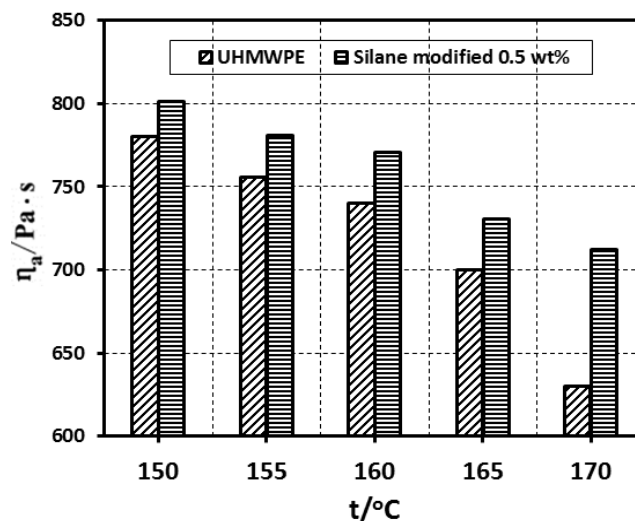


Figure 6: The impact of temperature on UHMWPE/modified nano-ZnO composites' melts viscosity ( $\gamma = 242.3 \text{ s}^{-1}$ )

## CONCLUSION

In this study, compression molding was used to generate UHMWPE/modified nano-ZnO nanocomposites with low doped nano-ZnO concentration utilizing UHMWPE and 3-aminopropyltriethoxy silane coupling agent-modified nano-ZnO. The mechanical and melt

rheological properties of the nanocomposites were evaluated using a capillary rheometer and a universal material testing equipment. Additionally, the plate-counting method was employed for the antimicrobial test. The investigation at hand could lead to the following conclusions:

Haydar U Zaman & Ruhai A Khan

- a) ZnO nanoparticles have improved the UHMWPE's mechanical attributes, such as its micro-hardness and compression characteristics. At 0.5 weight percent nano-ZnO filler loading, the maximum compressive strength is observed.
- b) Compressive modulus, tensile modulus, and Vickers micro-hardness of the nano-ZnO/UHMWPE nanocomposites all rose with increasing filler loading. Nano-ZnO was added, but the tensile strength and elongation at break of UHMWPE were reduced.
- c) According to the antibacterial test results, the modified nano-low ZnO's doping content would give the nanocomposites a favorable action against both *S. aureus* and *E. coli*.
- d) The melts of the nanocomposite display pseudoplastic behavior in accordance with the capillary rheological test. The low doped level of modified nano-ZnO in the UHMWPE matrix did not considerably affect the processability of the UHMWPE nanocomposites, as evidenced by the finding that the melt viscosity only slightly increased as the nano-ZnO content rose.

## REFERENCES

- [1] Abadi, M.B.H., Ghasemi, I., Khavandi, A., Shokrgozar, M., Farokhi, M., Homaeigohar, S.S., Eslamifar, A., 2010. Synthesis of nano  $\beta$ -TCP and the effects on the mechanical and biological properties of  $\beta$ -TCP/HDPE/UHMWPE nanocomposites, *Polymer Composites*. 31, 1745-1753.
- [2] Kurtz, S.M.: *The UHMWPE handbook: ultra-high molecular weight polyethylene in total joint replacement*: Elsevier, 2004.
- [3] Stein, H.L., 1988. Ultra high molecular weight polyethylene (UHMWPE), *Engineering Materials Handbook*. 2, 167-171.
- [4] Chan, C.-M., Wu, J., Li, J.-X., Cheung, Y.-K., 2002. Polypropylene/calcium carbonate nanocomposites, *Polymer*. 43, 2981-2992.
- [5] Zaman, H.U., Khan, R.A., 2022. Preparation and Evaluation of Polypropylene-Peanut Shell Flour Eco-Friendly Composites with and without Cloisite 30B, *Int. J. Adv. Sci. Eng.* 9, 2658-2668.
- [6] Zaman, H.U., Khan, R.A., 2022. Surface Modified Calotropis Gigantea Fiber Reinforced Polypropylene Composites, *Int. J. Adv. Sci. Eng.* 9 (1), 2477-2487.
- [7] Zaman, H.U., Ruhul Amin, 2022. Effects of Cloisite 20A Dispersion on the Structure and Properties of LDPE/Modified Clay/Coupling Agent Ternary Nanocomposites, *Int. J. Adv. Sci. Eng.* 8, 2341-2349.
- [8] Wang, Q., Xue, Q., Liu, H., Shen, W., Xu, J., 1996. The effect of particle size of nanometer ZrO<sub>2</sub> on the tribological behaviour of PEEK, *Wear*. 198, 216-219.
- [9] Wang, Q., Xue, Q., Shen, W., 1997. The friction and wear properties of nanometre SiO<sub>2</sub> filled polyetheretherketone, *Tribology International*. 30, 193-197.
- [10] Zhang, H.-J., Zhang, Z.-Z., Guo, F., Jiang, W., Wang, K., 2010. Surface modification of CuS nanoparticles and their effect on the tribological properties of hybrid PTFE/kevlar fabric/phenolic composite, *Journal of Composite Materials*. 44, 2461-2472.
- [11] Zaman, H.U., Hun, P.D., Khan, R.A., Yoon, K.-B., 2012. Morphology, mechanical, and crystallization behaviors of micro-and nano-ZnO filled polypropylene composites, *Journal of Reinforced Plastics and Composites*. 31, 323-329.
- [12] Bahadur, S., Sunkara, C., 2005. Effect of transfer film structure, composition and bonding on the tribological behavior of polyphenylene sulfide filled with nano particles of TiO<sub>2</sub>, ZnO, CuO and SiC, *Wear*. 258, 1411-1421.
- [13] Demjén, Z., Pukánszky, B., Nagy, J., 1998. Evaluation of interfacial interaction in polypropylene/surface treated CaCO<sub>3</sub> composites, *Composites Part A: Applied Science and Manufacturing*. 29, 323-329.
- [14] Sun, L., Ye, Z., Ma, L., Zhang, Y., 2022. Improving field emission performance of patterned ZnO electron emission source by optimizing array spacing, *Vacuum*. 201, 111-121.
- [15] Khan, R., Khan, M.I., Almesfer, M.K., Elkhaleefa, A., Ali, I.H., Ullah, A., Rahman, N., Sohail, M., Khan, A.A., Khan, A., 2022. The structural and dilute magnetic properties of (Co, Li) co-doped-ZnO semiconductor nanoparticles, *MRS Communications*. 12, 154-159.
- [16] Wang, Y., Hou, Z., Li, J., Wu, K., Song, J., Chen, R., Li, K., Hao, L., Xu, C., 2021. Simultaneously enhanced potential gradient and nonlinearity of ZnO varistor ceramics by MnO doping with nano-sized ZnO powders, *Materials*. 14, 7748.

Haydar U Zaman & Ruhul A Khan



- [17] Kang, Y., Yu, F., Zhang, L., Wang, W., Chen, L., Li, Y., 2021. Review of ZnO-based nanomaterials in gas sensors, Solid State Ionics. 360, 115544.
- [18] Bhunia, R., Das, S., Dalui, S., Hussain, S., Paul, R., Bhar, R., Pal, A.K., 2016. Flexible nano-ZnO/polyvinylidene difluoride piezoelectric composite films as energy harvester, Applied Physics A. 122, 1-13.
- [19] Pare, B., Barde, V.S., Solanki, V.S., Agarwal, N., Yadav, V.K., Alam, M.M., Gacem, A., Alsufyani, T., Khedher, N.B., Park, J.-W., 2022. Green Synthesis and Characterization of LED-Irradiation-Responsive Nano ZnO Catalyst and Photocatalytic Mineralization of Malachite Green Dye, Water. 14, 3221.
- [20] Li, S.C., Li, Y.N., 2010. Mechanical and antibacterial properties of modified nano-ZnO/high-density polyethylene composite films with a low doped content of nano-ZnO, Journal of Applied Polymer Science. 116, 2965-2969.
- [21] Zhang, L., Ding, Y., Povey, M., York, D., 2008. ZnO nanofluids-A potential antibacterial agent, Progress in Natural Science. 18, 939-944.
- [22] Liu, Y.-j., He, L.-l., Mustapha, A., Li, H., Hu, Z., Lin, M.-s., 2009. Antibacterial activities of zinc oxide nanoparticles against Escherichia coli O157: H7, Journal of Applied Microbiology. 107, 1193-1201.
- [23] Li, R., Yabe, S., Yamashita, M., Momose, S., Yoshida, S., Yin, S., Sato, T., 2002. UV-shielding properties of zinc oxide-doped ceria fine powders derived via soft solution chemical routes, Materials Chemistry and Physics. 75, 39-44.
- [24] Wu, R., Xie, C., Xia, H., Hu, J., Wang, A., 2000. The thermal physical formation of ZnO nanoparticles and their morphology, Journal of Crystal Growth. 217, 274-280.
- [25] Chandramouleeswaran, S., Mhaske, S., Kathe, A., Varadarajan, P., Prasad, V., Vigneshwaran, N., 2007. Functional behaviour of polypropylene/ZnO-soluble starch nanocomposites, Nanotechnology. 18, 385702.
- [26] Li, S.-C., Li, B., Qin, Z.-J., 2010. The effect of the Nano-ZnO concentration on the mechanical, antibacterial and melt rheological properties of LLDPE/modified Nano-ZnO composite films, Polymer-Plastics Technology and Engineering. 49, 1334-1338.
- [27] Zaman H.U., Khan, R.A., 2022. Substantial Enrichment of Mechanical, Thermal and Electrical Properties of Thermoplastic Polyester Elastomer by Melt Blending with Nano-ZnO. Emerging Trends in chemical Engineering. 9, 13-23.
- [28] Patil, S., Pawar, S., Chougule, M., Raut, B., Godse, P., Sen, S., Patil, V., 2012. Structural, morphological, optical, and electrical properties of PANi-ZnO nanocomposites, International Journal of Polymeric Materials. 61, 809-820.
- [29] Wang, J., Huang, N., Yang, P., Leng, Y., Sun, H., Liu, Z., Chu, P., 2004. The effects of amorphous carbon films deposited on polyethylene terephthalate on bacterial adhesion, Biomaterials. 25, 3163-3170.
- [30] Zhang, W., Chu, P.K., Ji, J., Zhang, Y., Fu, R.K., Yan, Q., 2006. Antibacterial properties of plasma-modified and triclosan or bronopol coated polyethylene, Polymer. 47, 931-936.
- [31] Han, C.D.: Rheology in polymer processing: Academic Press, 1976.
- [32] Sun, Y., Zhang, Z., Wong, C., 2005. Study on mono-dispersed nano-size silica by surface modification for underfill applications, Journal of Colloid and Interface Science. 292, 436-444.
- [33] Sawai, J., Kojima, H., Igarashi, H., Hashimoto, A., Shoji, S., Sawaki, T., Hakoda, A., Kawada, E., Kokugan, T., Shimizu, M., 2000. Antibacterial characteristics of magnesium oxide powder, World Journal of Microbiology and Biotechnology. 16, 187-194.
- [34] Dealy, J.M., Wissbrun, K.F.: Melt rheology and its role in plastics processing: theory and applications: Springer Science & Business Media, 2012.
- [35] Sun, S., Li, C., Zhang, L., Du, H., Burnell-Gray, J., 2006. Effects of surface modification of fumed silica on interfacial structures and mechanical properties of poly (vinyl chloride) composites, European Polymer Journal. 42, 1643-1652.